IEEE Access
Multidisciplinary | Rapid Review | Open Access Journal

Received May 8, 2020, accepted May 27, 2020, date of publication June 3, 2020, date of current version June 15, 2020.

Digital Object Identifier 10.1109/ACCESS.2020.2999511

Dual-Sensing System for Monitoring Ion Concentration Change in Electrochemical Micro Machining

CHUANJUN ZHAO AND LIZHONG XU
Mechanical Engineering School, Yanshan University, Qinhuangdao 066004, China
Corresponding author: Lizhong Xu (xlz@ysu.edu.cn)

ABSTRACT Currently, no reliable electrolyte concentration monitoring method exists for ultra-short pulsed electrochemical micromachining. A dual-sensing system for electrolyte concentration monitoring is proposed in this work. An inductance element is added into the classical pulsed electrochemical micromachining circuit system. For it, a modified circuit equation is proposed by which the coupled electronic and ion circuit is analyzed, and two modes of the coupled circuit are found. The asynchronous mode is used to monitor the concentration changes of the ions in electromechanical micromachining, and a novel method of electrolyte concentration monitoring is obtained. Combining this method with the short-circuit frequency monitoring method, an electrolyte concentration monitoring method based on the dual-sensing monitoring system is proposed, and corresponding monitoring software is produced. The software is used in actual microstructure processing experiments, obtaining nanometer-scale machining accuracy.

INDEX TERMS Dual sensing system, monitoring ion concentration, electrochemistry, micro machining.

I. INTRODUCTION

Electrochemical machining (ECM) technology using ultra-short pulses was proposed by Schuster *et al.* [1], and developed using the results obtained from the tip electrode of the microscope [2], [3]. ECM technology has received extensive attention due to its unique advantages.

For ECM technology, various simulation methods have been proposed. A multi-physics simulation was carried out, and cathode optimization was completed to improve the accuracy of the inner-walled ring grooves [4]. A multi-physics model was proposed to model the temperature evolution in the pulsed electrochemical machining process [5]. Another multi-physical model was used to describe the influence of pulse parameters on the conductivity distribution of the electrolyte [6]. The optimized pulse duty cycle, average voltage, and short duration of pulse voltage were adopted to increase the machining accuracy of the microelements [7], [8]. Tool electrode shape was improved to reduce the taper of the produced microstructure [9]. A numerical method considering the inductance of the power supply circuit was proposed to study the influence of inductance on the voltage pulse during machining [10]. For pulsed electrochemical machining, tool cathode vibration technology was used to increase the machining quality of the produced microelements [11]. Novel control circuits of the micromachining system were proposed to increase the machining accuracy of the technology [12]–[14]. Neural networks and fuzzy logic control methods were investigated in pulsed electrochemical machining [15], [16]. A model predictive control approach was also used in the machining technology [17]. The tool electrode short-circuit frequency monitoring method was used to monitor the operation state of the machining system for ensuring the processing quality of the ECM technology [18]–[22].

To summarize, a lot of studies have focused on ultra-short pulsed electrochemical micromachining. However, to ensure machining accuracy, the electrochemical reaction speed must have good controllability. The electrochemical reaction speed of electrolytes in a general concentration is too fast to meet the machining precision requirements of the microstructure. Therefore, the electrolyte concentration and amount is very low during the process. As the concentration changes quickly, it is necessary to timely supplement an appropriate amount of electrolyte. Therefore, concentration monitoring of the electrolyte is necessary. In the studies above, the ion concentration change has seldom been considered.

The associate editor coordinating the review of this manuscript and approving it for publication was Jing Liang.

Short-circuit frequency monitoring has not completely solved the concentration monitoring problem because in addition to the decrease in electrolyte concentration, low voltage and fast feed speed also lead to an increase of short circuit times. There is currently no reliable electrolyte concentration monitoring method in electrochemical micromachining.

Therefore, this paper proposes an electrolyte concentration monitoring method based on a dual sensing system. Firstly, an inductance element is added into the classical pulsed electrochemical micromachining circuit system. For the circuit system, a modified circuit equation is proposed. By the modified equation, the modes of the coupled electronic and ion circuit are analyzed, and two modes of the coupled circuit are found (asynchrony and synchronous modes). Then, the asynchronous mode is used to monitor the concentration changes of the ions in electromechanical micromachining. Finally, combining this monitoring method with the short-circuit frequency monitoring method, an electrolyte concentration monitoring method based on the dual-sensing monitoring system is proposed, and the corresponding monitoring software is produced. The software is then used in microstructure machining to obtain nanometer-scale machining accuracy.

II. TWO MODES IN COUPLED ELECTRONIC AND ION CIRCUIT

An inductance element was added in the circuit of the electrochemical reaction to develop a coupled ion-electronic circuit. A pulse voltage was applied to this circuit. The voltage response was measured between the two electric poles of the electrochemical system.

The voltage responses between the two electric poles were evaluated using two modes (Fig. 1). In the first mode, the inductance element was directly connected to the ground, and the other pole was linked to a positive or negative voltage (mode A). For the second mode, the inductance element was directly connected to a positive or negative voltage, and the other pole was connected to the ground (mode B).

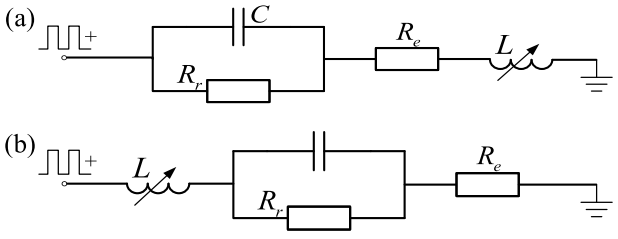

FIGURE 1. Coupled ion-electric circuit. (a)mode A; (b)mode B.

A cylindrical W wire 10 μm in diameter was used as a cathode while a nickel plate was employed as an anode, and 0.1 M H_2SO_4 was used as an electrolyte. The inductance in the electric circuit was taken as 5 mH. The amplitude of the pulse signals was 1 V, and the frequency of the pulse signals was 30 kHz. The voltage responses between the two electric poles to the pulse signals were measured using an oscilloscope, where the response signals were fed into a computer for display (see Fig. 2).

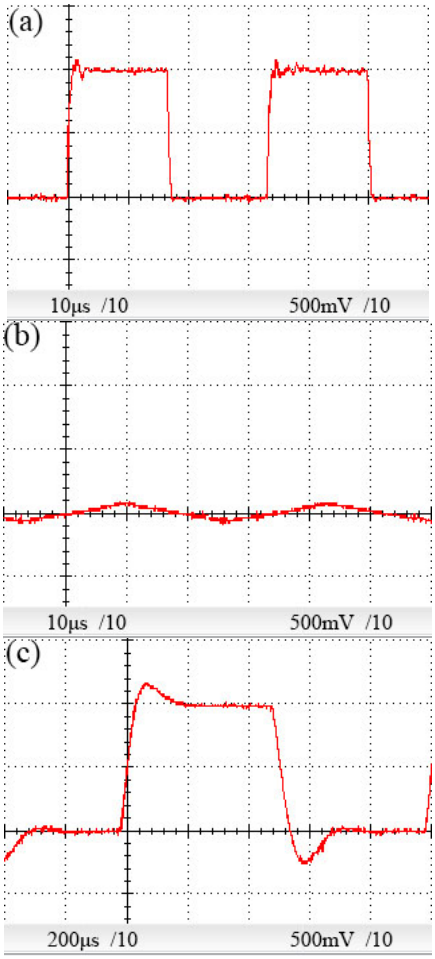

FIGURE 2. Voltage responses between two electric poles. (a) inductance element is directly connected to the ground, mode A (30 kHz and 5 mH); (b) inductance element is connected to a positive or negative voltage, mode B (30 kHz and 5 mH); (c) mode B, 1 kHz and 5mH.

The results showed that the voltage responses under the two given situations were completely different from each other even if both the inductance element and ion circuit were identical to each other.

For mode A, the voltage response was a typical waveform of the two-order oscillation system, which coincided with the analysis using the classical control theory of the two-order oscillation system.

For mode B, the voltage response between the two electric poles to pulse voltage was in conflict with the analysis in the classical control theory. Its amplitude was greatly reduced, while its response time was significantly increased. In a given inductance (5 mH), the frequency of the step voltage signals were reduced from 30 to 1 kHz. Overshoot above the pulse voltage was then observed, with a response time of about 40 μs. This was 40 times the response time (1 μs) for mode A. Hence, the response time of mode B was hugely increased compared to mode A.

III. ANALYSIS OF THE VOLTAGE RESPONSES FOR TWO MODES

For mode A, the pulse voltage was initially applied to the double layers of the ion circuit. After the responses of the ion circuit, the pulse voltage was transmitted to the electronic circuit of the inductance element. In this case, the start-up of the electronic current was much faster compared to the ion circuit. As the ion circuit current began, the electronic circuit current was initiated quite quickly, and the start-up of the two circuits was almost synchronous. Thus, it was an oscillation circuit that consisted of inductance, capacitance, and resistance. The oscillation equation is [14]:

$$LC\frac{d^2\varphi}{dt^2} + R_eC\frac{d\varphi}{dt} + \varphi = \Phi \tag{1}$$

where L is the inductance; Φ is the step voltage applied to the circuit; φ is the DL (double layers) polarization voltage; R_e is the electrolyte resistance ($R_e = \rho d/S$); ρ is the specific electrolyte resistivity; d is the local separation between electrodes; C is the DL capacitance in the ion circuit ($C = C_dS$, C_d is DL capacitance per unit area, S is the area of the partial electrode where the electrochemical reaction occurs); and t is the time. Here, R_r is the electrochemical reaction resistance, and as its value is too large to influence the performance of the circuit, it is neglected [13].

In the micro electrochemical system, the separation between the electrodes is small, which makes the electrolyte resistance also quite small. This means that an owe damping state occurs in the equivalent circuit. When applying the step voltage pulse, a voltage peak larger than the stable step voltage will be created. Then, it will attenuate to the stable voltage value as reflected by the gathered results in Fig. 2(a).

Although the relative damping factor, $\xi = \frac{R_e}{2}\sqrt{\frac{C}{L}}$ reduces with the inductance L, the peak time ($t_p = \frac{\pi}{\omega_n\sqrt{1-\xi^2}}$) increases because the natural frequency $\omega_n = \sqrt{\frac{1}{LC}}$ of the coupled circuit reduces with the inductance. Hence, the voltage peak of the pulse responses becomes bigger, and the time corresponding to the voltage peak becomes longer with increased inductance.

For mode B, the electronic circuit current was initially started, but the pulse voltage could not be simultaneously transmitted to the ion circuit.

For mode A, although the response time of the ion circuit was also slow, after the voltage of the ion circuit reached the peak, the voltage of the electronic circuit could also reach the peak almost at the same time. For mode B, the voltage peak of the electronic circuit was first reached, then the voltage peak of the ionic circuit was reached more slowly. That is, the time for the two circuits to reach the voltage peaks was not synchronized.

For mode A, the time for two circuits to reach the voltage peaks was nearly synchronized. For mode B, the time for two circuits to reach the voltage peaks was not synchronized. Thus, the time when the ion circuit reaches the voltage peak had a certain delay.

The start-up of the electronic current was much quicker than the ion circuit. After the responses of the electronic circuit current, the ion circuit current could be started following a time delay. Therefore, the pulsed response between the two poles did not adhere to Eq. (1). To identify the pulsed response, Eq. (1) is expressed as:

$$LC\frac{d^2\varphi(t)}{dt^2} + R_eC\frac{d\varphi(t-\tau)}{dt} + \varphi(t) = \Phi(t) \tag{2}$$

where τ represents the time delay between the ion and electronic circuits.

The time delay can be expressed by the equation,$e^{-\tau s} \approx 1 - \tau s$. Substituting the time delay equation into Eq. (2), produces:

$$[LCs^2 + R_eCs(1-\tau s) + 1]\varphi(s) = \Phi(s) \tag{3}$$

Equation. (3) can be modified into the following form:

$$[(LC - \tau R_eC)s^2 + R_eCs + 1]\varphi(s) = \Phi(s) \tag{4}$$

From Eq. (4), the equivalent damping factor of the coupled fluid-electric circuit can be obtained as shown below:

$$\xi = \frac{R_e}{2}\sqrt{\frac{C}{L}}\frac{1}{\sqrt{1 - R\tau/L}} \tag{5}$$

Equation (5) shows that the time delay increases the equivalent damping factor for the coupled circuit. It largely prolongs the response time of the circuit to step voltage.

The pulsed response between the two poles was simulated using Eq. (4) (see Fig. 3). Figure 3a shows that the simulation agreed with the measured results in Fig. 2b. The similarity between the simulation and measurement validates earlier speculation regarding the asynchrony of both the electronic circuit and the ion circuit currents.

Figure 3 shows that the circuit time delay was equivalent to the partial damping. This made the response time of the equivalent circuit system longer. Above this, the voltage response between the two poles increased gradually in time, but could not achieve the voltage peak during the pulse voltage for the limited pulse duration of the source voltage. As the pulse voltage stopped, the voltage response was gradually reduced. In this case, the duty cycle was divided into half, while the voltage response could not be reduced to zero until the other step voltage was applied to the coupled circuit.

If the duty cycle of the step voltage signals is taken as 1/10, the voltage response between the two poles increases gradually with time and also does not reach the voltage peak during the pulse voltage for the limited pulse duration of the source voltage. As the pulse voltage stops, the voltage response could be gradually reduced to zero.

To analyze the asynchrony between the electronic circuit current and the ion circuit current, an identified circuit was created (Fig. 4). The two resistances can be seen at the two sides of the ion circuit (point line).

A cylindrical W wire 10 μm in diameter was used as a cathode while the nickel plate was held as an anode, and 0.1 M

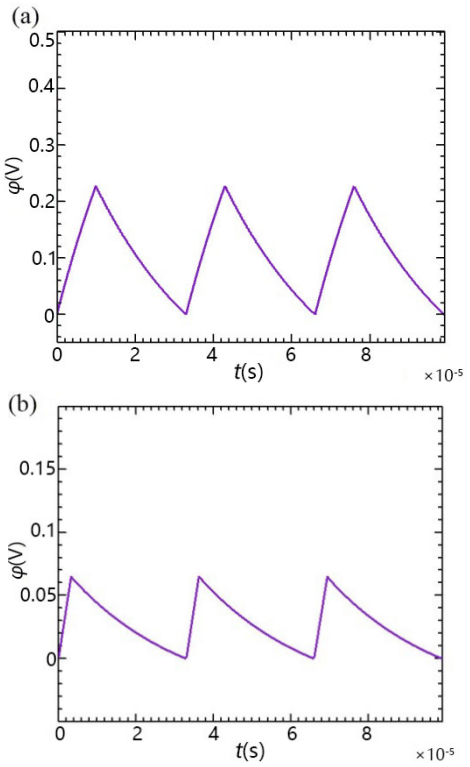

FIGURE 3. Simulated pulsed responses between two poles. Here, frequency of the step voltage signals is 30 kHz, voltage peak is 1V; inductance L=5 mH, time delay τ is 23 ns.(a). duty cycle is 1/2; (b). duty cycle is 1/10.

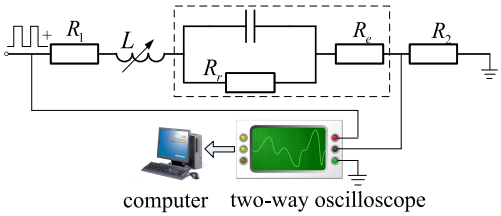

FIGURE 4. Detected circuit for the asynchrony between the electronic and ion currents.

H_2SO_4 was used as the electrolyte. The peak of the pulse signals was 500 mV, the frequencies of the pulse signals were taken as 1 MHz, 500 kHz, and 100 kHz, respectively, and the pulse-to-pause ratio was 50%. The inductance in the electric circuit was 0 mH (no inductance) and the electric current responses on the two electric resistances to the pulse signals were measured using a two-way oscilloscope (Fig. 5). In this figure, the following is shown:

Generally, asynchrony between the electronic circuit current and the ion circuit current was observed. The ion circuit current was slower compared to the electronic circuit current. For the different frequencies of the voltage signals, the time delay was identical. The measured average time delay was about 23 ns. The results verify the initial speculation and analysis about the asynchrony between the electronic circuit current and the ion circuit current. This shows that the time

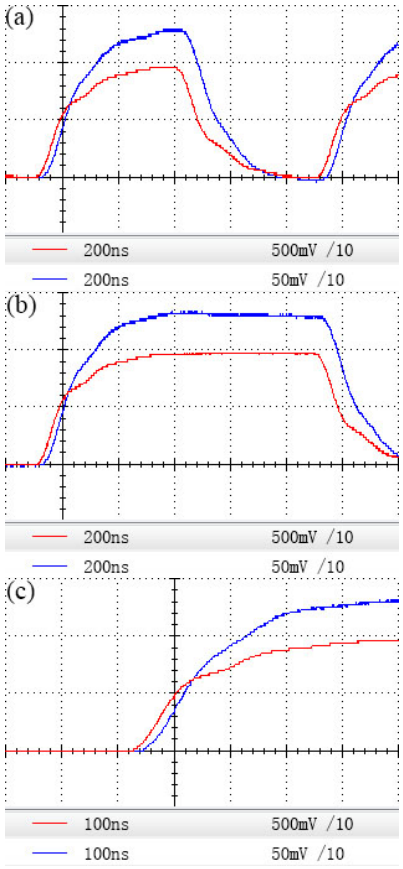

FIGURE 5. Asynchrony between the electronic and ion currents; (a).1 MHz; (b).500kHz;(c).100 kHz; red line: before ion circuit; blue line: after ion circuit.

delay of the circuit is similar to the partial damping, causing the response time of the equivalent circuit system to be longer.

To summarize, the two current modes of the coupled ion-electronic circuit were identified as asynchronous and synchronous modes. Based on the results, the peak voltage of the pulse responses increases, and the time related to the voltage peak becomes long when inductance is raised during the synchronous mode. Meanwhile, the synchronous mode is used in electrochemical micromachining through pulse current, and increases the machining resolution of the microstructure by tuning the inductance. As seen in the asynchronous mode, the changes in the relative damping coefficient are quite visible. This can be used to identify the parameters directly related to the damping, such as ion concentration. It can also be employed to check the electrochemical micromachining system by monitoring the ion concentration changes.

IV. ANALYSIS OF THE VOLTAGE RESPONSES FOR TWO MODES

Mode A is used for electrochemical micromachining [19]. Here, mode B (asynchronous mode) was used to monitor the ion concentration change in the electrochemical micromachining. The two monitor poles were linked to the coupled

ion-electronic circuit with an adjustable inductance. The inductance element was not connected to the ground, while the other end of the coupled circuit was connected to the ground (Fig. 6). The measured voltage responses between the two poles for the different ion concentrations showed the following:

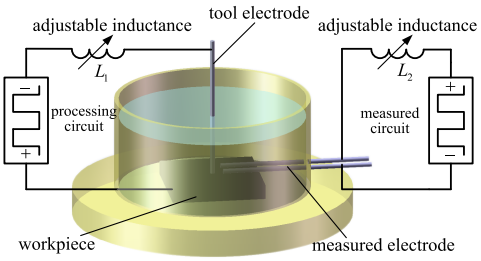

FIGURE 6. Monitor of the ion concentration change in electrochemical micro machining.

When the concentration of the sulfuric acid solution was reduced, the time of the voltage responses between the two poles was also reduced. There was a distinct connection between the time of the voltage responses and the solution resistance for the asynchronous mode. In Eq. (4), the natural frequency of the coupled circuit is shown as:

$$\omega_n = \sqrt{\frac{1}{LC - \tau R_e C}}$$

Also, when the concentration of the sulfuric acid solution was reduced, the damping constant of the solution increased, which raised the solution resistance (Re). Using the equation, it can be seen that the natural frequency of the coupled circuit increases along with it. This makes the voltage response time decrease.

In Eq. (5), it is shown that the damping constant can be reduced by increasing the inductance (L). However, the natural frequency of the coupled circuit is much smaller compared to mode A. This makes the voltage response time much longer in mode A.

The concentration change of the sulfuric acid solution can be identified through the voltage response time-inductance relationship or the voltage response time. The detection process that uses the voltage response time is relatively easy, which enables this method to be widely used in most studies [6], [18], [19].

In Fig. 6, a pair of W poles with 0.1 mm in diameter and 1 mm distance were used as the detection pole to monitor the ion concentration change in electrochemical micromachining. The detection pole was near the tool pole, but they had no contact with each other. Thus, the ion concentration change near the tool pole could be observed in real time.

The measured voltage response signals between the two poles were input into the computer using a filter and an acquisition card (PCI-1710UL, 100 kS/s, see Fig. 7). In the programming, the peak time of the measured voltage response signals between two poles could be calculated, including their

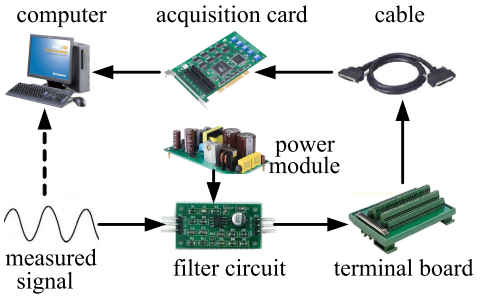

FIGURE 7. Composition of the monitoring circuit.

output. The peak time changes show the ion concentration changes in electrochemical micromachining.

The pulse voltage frequency of the machining circuit was 30 kHz while its amplitude was 1.1 V. In the detection circuit, the pulse voltage frequency was 100 Hz, while its amplitude was 280 mV. The pulse voltage frequency of the detection circuit was taken to be a small value, which can cause a large peak time change for a given ion concentration. Thus, high sensitivity of the peak time to ion concentration could be obtained. Meanwhile, the pulse voltage amplitude of the detection circuit was seen to have minimal value when reducing its effects on the machining circuit. To eliminate the effects of the high-frequency machining signals in the detection signals, a low pass filter (with a cut-off frequency of 3 kHz) was used.

Identifying the program in the computer mainly consisted of data collection, background data processing, and peak time calculation.

In the detection system of the electrochemical micromachining, the data acquisition card PCI-1243U was used. The card sampling rate was 100 kS/s, which could keep the processing voltage record in a timely manner. This means that 100,000 data were obtained per second. Thus, the acquisition time for one datum was 10 μs. The pulse voltage frequency of the detection circuit was 100 Hz, while its time period was 10 ms. In order to determine the accurate peak time of the detected signals, two time periods (20 ms) of the detected signals were required. This means 2000 data was needed. In reducing the background data processing time, the acquisition number was taken to be 2000, and the buffering storage zone (through first in, first out [FIFO] method) in the acquisition card was used, which was 2000 (2048).

The background data processing follows three steps. First, it searches for the voltage peak by identifying the maximum voltage in 2000 data, where both voltage and current achieve the maximum value (i_{max}, V_{max}). Second, it finds the zero voltage points by starting to identify the maximum value (i_{max}, V_{max}) to frontal data and for reaching the first zero voltage point (i_{min}, 0). Third, it calculates the peak time t_p (Figs. 8-9).

To increase the detection accuracy of the peak time, the average value should be over 10 times that of the calculation in the output (Fig. 12a). In this figure, the left image

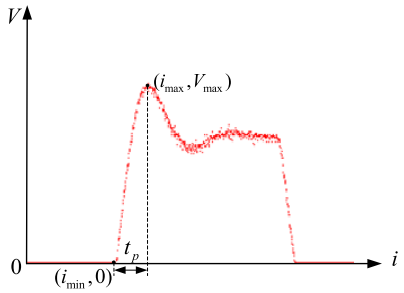

FIGURE 8. Search for typical voltage points.

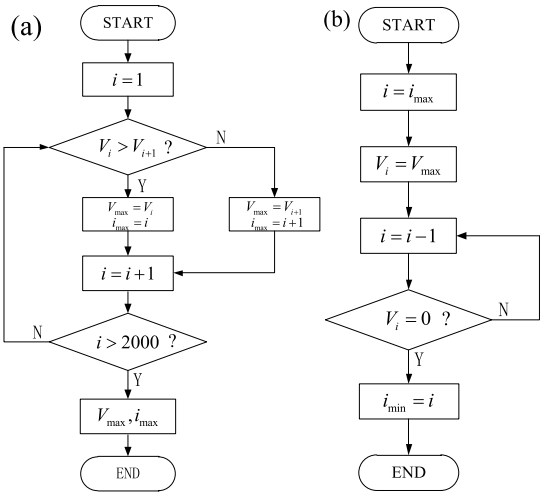

FIGURE 9. Voltage peak and zero voltage searches; (a). voltage peak search; (b).zero voltage search.

shows the initial measurement results, while the right figure is the real-time changes in the peak time. In the face plate when setting the sampling parameters, the sampling mode, sampling rate, sampling number, and FIFO size can be selected. The right image is the detailed data in a table that provides the measured peak voltage time.

The relationship between the peak time and the concentration of the sulfuric acid solution can then be evaluated.

First, in a non-processed state (voltage was applied to measured poles, and not applied to tool poles), the peak time for three different concentrations of the sulfuric acid solution was detected (see Fig. 10a). Figure 10a shows that the change of the peak time being measured was about 80 μs when the concentration in the sulfuric acid solution was converted from 0.03 to 0.01 M. This means that a 0.005 M concentration change was linked to 20 μs change in the peak time. Then, in a processed state (voltages were applied to both measured poles and tool poles), the peak time changed for three different concentrations of the sulfuric acid solution detected before and after applying voltage on tool electrode (see Figs. 10b, 10c, and 10d). In the figures, the left bottom curve shows the state applied voltage to detection poles, and the right top curve is for the state applied voltage to both detection poles and machining poles.

Figures 10b, 10c, and 10d highlight that the peak time increased significantly as the voltage was applied to the tool poles. However, the change of the peak time under machining was identical to one for the state when the voltage was only applied to the detection poles. This shows that the change of the peak time was still about 80 μs when the concentration in the sulfuric acid solution changed from 0.03 to 0.01 M, meaning that a 0.005 M concentration change still corresponded to about 20 μs change in the response time.

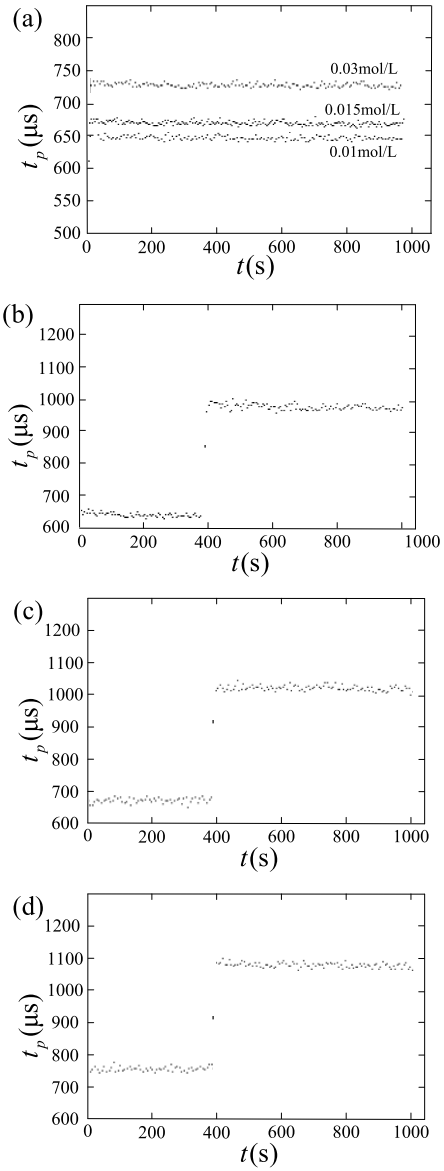

FIGURE 10. Measured peak time t_p for different concentrations of sulfuric acid; (a). in non-processed state; (b). in processed state for 0.01 M sulfuric acid; (c). in processed state for 0.015 M sulfuric acid; (d). in processed state for 0.03.

The peak time t_p and time difference Δt_p for three different concentrations of the sulfuric acid solution are given in Table 1 (here, Δt_p is equal to the difference between two adjacent voltage response time t_p). It shows that in processed

TABLE 1. PEAK time changes for different ion concentration.

c(mol/L)	t_p(μs, processed state)	t_p(μs, non-processed state)	Δt_p (μs)
0.01	650	990	25
0.015	670	1020	60
0.03	730	1080	

state, peak time difference for different concentrations of the sulfuric acid solution was identical to that in a non-processed state. Therefore, the detection system can be calibrated in a non-processed state, and then used to detect ion concentration change in a processed state.

When monitoring the changes of the peak time, the concentration modifications of the ions in the cited electromechanical micromachining are checked (Fig. 11). By doing so, a detecting system for the peak time change during micromachining is developed. Initially, the detection system is turned on and then the tool and workpiece poles are applied with the voltage. Figure 11 shows the following.

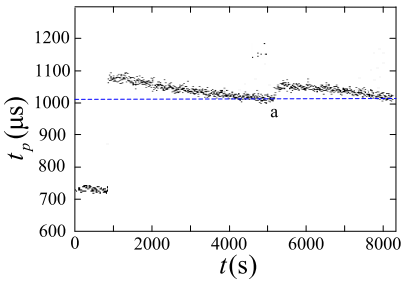

FIGURE 11. Changes of the voltage peak time during machining.

As the detection system is turned on prior to applying the machining voltage, the peak time deteriorates and its average values become relatively small. When the machining voltage is turned on, the sudden increase of the peak time occurs and fluctuates at a relatively large average value. The reason behind is that most of the ions move near to the tool pole when the voltage is applied to it and the ion concentration near the detection poles also becomes large (the detection poles are near to the tool pole).

In carrying out the micromachining, a gradual decline in the peak time occurs. This shows that the ion concentration slowly decreases in the electrolytic cell. When the machining is sustained, the peak time of the voltage is reduced, where the ion concentration is further reduced.

As the peak time was reduced from 1080 to 1020 μs, the short-circuit times began to increase (58 times that of the short-circuit occurred at point a), and the machining ability of the system visibly declined. Here, the ion concentration in the sulfuric acid solution was reduced from 0.03 to 0.015 M. The results show the following:

Once the peak time of the voltage decreased to 94% of its initial value (1020 μs), the ion concentration in the sulfuric acid solution had been reduced by 50% of its initial concentration (0.03 M). The results show that when the peak time of the voltage declined by 6% of its initial response time, the machining ability was reduced significantly, and its machining quality could not be ensured.

Therefore, electrolyte supplementation should be carried out in a timely manner. This is done by adding a bit of electrolyte during the danger time (a point) while the peak time of the voltage is suddenly increased. Thus, the micromachining can be sustained as the gradual decrease of peak time reoccurs.

V. MONITOR ION CONCENTRATION CHANGE BASED ON DOUBLE SENSOR SYSTEM

In order to ensure the reliability of the concentration monitoring system in the electrochemical micromachining process, a dual-sensing concentration monitoring system based on peak time sensing and short-circuit frequency sensing was constructed.

Here, the short-circuit frequency monitoring system based on a Hall current sensor was used to detect the change of machining circuit current in real time. The Hall sensor can convert the current change of the machining circuit into voltage change and transmit the data to the computer through a data acquisition card. A data acquisition card PCI-1710UL, with the sampling rate of 100 kS/s and the sampling resolution of 12 bits was selected, which could collect small changes of voltage value in real time. The acquisition card was able to realize multi-channel continuous data acquisition to fulfill the system's peak time detection and short-circuit detection simultaneously.

In the process of micro-electrochemical machining, the voltage signals from the Hall current sensor were at millivolt level, which is easily affected by external electrostatic interference, and thus affects the determination of the state of electrochemical machining. For it, an aluminum/mylar foil and braided copper double-shielded cable was used to prevent external interference from weakening electrical signals. As the voltage in micro electrochemical machining is usually below 2 V, the concentration of electrolyte used was also low, and the resistance of the electrolyte was large. As a result, the current in the machining circuit was very weak (usually at the microampere level), and the voltage converted by the Hall sensor was very small (usually at the millivolt level) during the normal micro-electrochemical machining. When a short circuit occurs in electrochemical machining, the tool electrode will contact the workpiece directly, the resistance will decrease sharply, and the current in the circuit will increase sharply. At this time, the voltage converted by the Hall sensor will also increase sharply and exceed the set short-circuit voltage value, and the system will judge the short-circuit state and calculate the short-circuit times. When the number of short-circuits exceeds 20 times per minute, it indicates that the dissolution speed in electrochemical machining is lower than the workpiece feeding speed.

There is no single reason why the dissolution rate of electrochemical machining is lower than the workpiece feed rate. It may be due to low ion concentration, or because the tool electrode feed rate is too fast.

Therefore, a dual-sensing concentration monitoring system based on peak time sensing and short-circuit frequency sensing is needed to monitor ion concentration. The proposed control interface is shown in Fig. 12(a), and the corresponding computer control block diagram of the dual-sensor system is shown in Fig. 12(b).

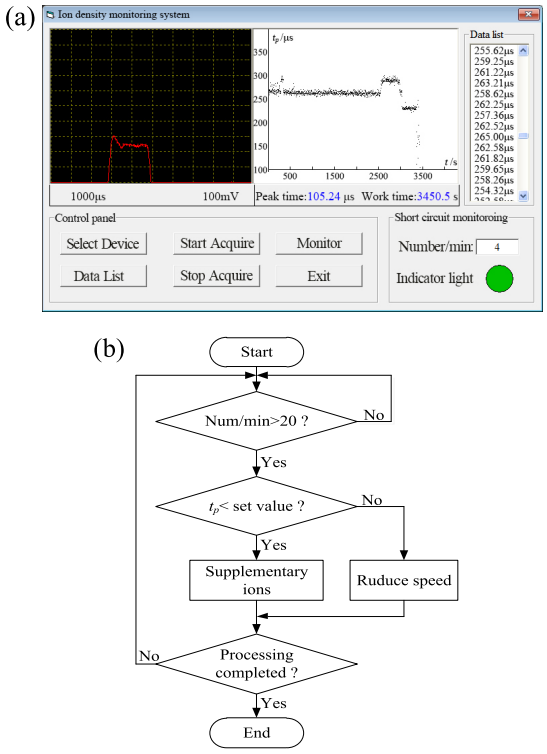

FIGURE 12. Dual-sensing concentration monitoring system. (a) Control interface; (b) Control block diagram.

When the monitor system is running, the data acquisition card carries out real-time data acquisition on the peak time and current in the system through two channels respectively. The internal program respectively carries on with the operation analysis and the processing of the data.

When the program is running, the monitoring system first monitors the short circuit frequency in electrochemical machining. When the short-circuit frequency is more than 10 times per minute, it indicates that the dissolution speed of electrochemical machining is lower than the workpiece feeding speed.

The state of electrochemical machining needs to be further judged according to the peak time change of the system. If the peak time change of the concentration sensing system is not lower than the set value, it indicates that the electrolyte concentration consumption is not high at that moment. This means that the initial setting speed should be higher than the current dissolution speed of the workpiece, and the processing feed will be reduced through the control program. On the contrary, if the peak time of the concentration sensing system changes significantly and is lower than the set value, it indicates that the concentration of electrolyte is being excessively consumed, and the system will supplement the electrolyte by controlling the operation of the micro-pump.

After the above steps, the program will judge whether the electrochemical machining is completed. If the machining is completed, the program will be terminated; otherwise, it will return to the short-circuit detection step and continue to run.

Acidic electrolytes are commonly used electrolytes in electrochemical micromachining. Among them, dilute sulfuric acid is the most widely used. Therefore, the ion concentration monitoring was carried out for dilute sulfuric acid solution in this work. During processing, the consumption of hydrogen ions and the production of nickel ions occurs simultaneously. The electrical conductivity of the hydrogen ions is much larger than that of the nickel ions. Therefore, the consumption of hydrogen ions during processing leads to the increase of electrolyte resistance and thus the peak time. What is monitored here is actually the decrease in hydrogen ion concentration.

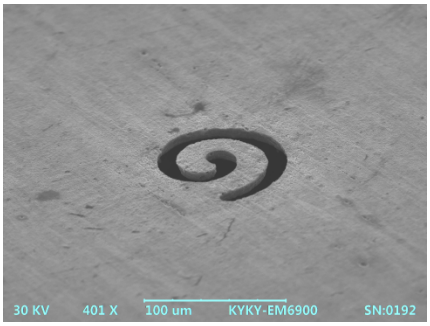

FIGURE 13. micro Archimedes spiral beam machined with double sensor system.

Figure 13 shows a micro Archimedes spiral beam produced using the proposed detection system. Here, a polished W wire 10 μm in diameter was used as tool, 0.1 M sulfuric acid was used as electrolyte, and the micro spiral beam was machined on mechanically polished Ni sheets. On the micro Archimedes spiral beam, the width of the trough was about 11 μm. The effective distance between the tool and the wall of the trough was about 500 nm. The machining accuracy was about four times higher than that in reference [4]. The well-defined shape and nanometer-scale precision of the micro spiral beam demonstrates the detection technique of the ion concentration during pulsed electrochemical micromachining.

VI. CONCLUSIONS

In this paper, an electrolyte concentration monitoring method based on a dual-sensing system was proposed. An inductance element was added into the classical pulsed electrochemical micromachining circuit system. For it, a modified

circuit equation was proposed by which the coupled electronic and ion circuit was analyzed, and two modes of the coupled circuit were found: the asynchronous and synchronous modes. In the asynchronous mode, the relative damping coefficient changes were quite visible. This could be used to identify the parameters related to the damping, such as ion concentration, etc. Here, the asynchronous mode was used to monitor the concentration changes of the ions in electromechanical micromachining, and a novel method of electrolyte concentration monitoring was given. Combining this method with the short-circuit frequency monitoring method, the electrolyte concentration monitoring method based on the dual-sensing system was proposed, and the corresponding monitoring software was produced. The system was then used in actual processing experiments of the microstructure, achieving nanometer-scale machining accuracy.

REFERENCES

[1] R. Schuster, V. KirchneV, X. Xia, A. M. Bittner, and G. Ertl, "Nanoscale electrochemistry," *Phys. Rev. Lett.*, vol. 80, no. 25, pp. 5599–5602. Jun. 1998.
[2] J. Kozak, D. Gulbinowicz, and Z. Gulbinowicz, "The mathematical modeling and computer simulation of pulse electrochemical micromachining using ultrashort pulses," *Eng. Lett.*, no. 16, pp. 556–561, Oct. 2008.
[3] R. Schuster, V. Kirchner, P. Allongue, and G. Ertl, "Electrochemical micromachining," *Science*, vol. 289, no. 5476, pp. 98–101, Jul. 2000.
[4] C. Zhang, H. Ai, Z. Yan, X. Jiang, P. Cheng, Y. Hu, and H. Tian, "Cathode optimization and multi-physics simulation of pulse electrochemical machining for small inner-walled ring grooves," *Int. J. Adv. Manuf. Technol.*, vol. 106, nos. 1–2, pp. 401–416, Jan. 2020.
[5] Y. Chen, M. Fang, and L. Jiang, "Multiphysics simulation of the material removal process in pulse electrochemical machining (PECM)," *Int. J. Adv. Manuf. Technol.*, vol. 91, nos. 5–8, pp. 2455–2464, Jul. 2017.
[6] M. Fang, Y. Chen, L. Jiang, Y. Su, and Y. Liang, "Optimal design of cathode based on iterative solution of multi-physical model in pulse electrochemical machining (PECM)," *Int. J. Adv. Manuf. Technol.*, vol. 105, nos. 7–8, pp. 3261–3270, Dec. 2019.
[7] W. Chen, F. Han, and J. Wang, "Influence of pulse waveform on machining accuracy in electrochemical machining," *Int. J. Adv. Manuf. Technol.*, vol. 96, nos. 1–4, pp. 1367–1375, Apr. 2018.
[8] M. Mithu, G. Fantoni, and J. Ciampi, "The effect of high frequency and duty cycle in electrochemical micro drilling," *Int. J. Adv. Manuf. Technol.*, vol. 55, nos. 9–12, pp. 921–933, Aug. 2011.
[9] Y. Wang, Y. Zeng, N. Qu, and D. Zhu, "Electrochemical micromachining of small tapered microstructures with sub-micro spherical tool," *Int. J. Adv. Manuf. Technol.*, vol. 84, nos. 5–8, pp. 851–859, May 2016.
[10] T. Koyano, A. Hosokawa, and T. Furumoto, "Analysis of electrochemical machining process with ultrashort pulses considering stray inductance of pulse power supply," *J. Adv. Mech. Des. Syst. Manuf.*, vol. 12, no. 5, pp. 1–10, Nov. 2018.
[11] X. Jiang, J. Liu, D. Zhu, M. Wang, and N. Qu, "Research on stagger coupling mode of pulse duration and tool vibration in electrochemical machining," *Appl. Sci.*, vol. 8, no. 8, p. 1296, Aug. 2018.
[12] L. Xu, X. Bai, and C. Zhao, "Communication—Electrochemical micromachining with adjustable resistance," *J. Electrochem. Soc.*, vol. 164, no. 14, pp. E572–E574, Dec. 2017.
[13] C. Zhao and L. Xu, "Pulse width tuning in electrochemical micromachining system," *IEEE Access*, vol. 8, pp. 23713–23719, 2020.
[14] L. Xu and C. Zhao, "Nanometer-scale accuracy electrochemical micromachining with adjustable inductance," *Electrochimica Acta*, vol. 248, pp. 75–78, Sep. 2017.
[15] G. Pang, W. Xu, X. Zhai, and J. Zhou, "Forecast and control of anode shape in electrochemical machining using neural network," *Adv. Neural Netw.*, vol. 3174, pp. 262–268, Aug. 2004.
[16] V. J. Keasberry, A. W. Labib, J. Atkinson, and H. W. Frost, "A fuzzy logic control approach to electrochemical machining (ECM)," in *Proc. 34th Int. MATADOR Conf.*, Jul. 2004, pp. 153–160.
[17] M. Boxhammer and S. Altmannshofer, "Model predictive control in pulsed electrochemical machining," *J. Process Control*, vol. 24, no. 1, pp. 296–303, Jan. 2014.
[18] E. L. Hotoiu and J. Deconinck, "A novel pulse shortcut strategy for simulating nano-second pulse electrochemical micro-machining," *J. Appl. Electrochemistry*, vol. 44, no. 11, pp. 1225–1238, Nov. 2014.
[19] W. Chen and F. Han, "Short-circuit avoidance in electrochemical machining based on polarization voltage during pulse off time," *Int. J. Adv. Manuf. Technol.*, vol. 102, nos. 5–8, pp. 2531–2539, Jun. 2019.
[20] Y. Liu, X. Wu, and H. Kong, "Investigation of electrochemical nanostructuring with ultrashort pulses by using nanoscale electrode," *Current Nanoscience*, vol. 15, no. 3, pp. 279–288, Feb. 2019.
[21] J. Zhao, Y. Lv, F. Wang, Z. Yang, D. Liu, Y. Fan, and Y. He, "Experimental research on process stability in pulsed electrochemical machining of deep narrow grooves with high length-width ratio," *Int. J. Adv. Manuf. Technol.*, vol. 96, nos. 5–8, pp. 2245–2256, May 2018.
[22] H. Demirtas, O. Yilmaz, and B. Kanber, "Controlling short circuiting, oxide layer and cavitation problems in electrochemical machining of freeform surfaces," *J. Mater. Process. Technol.*, vol. 262, pp. 585–596, Dec. 2018.

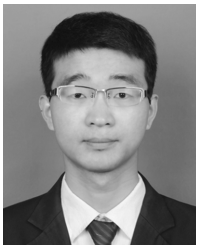

CHUANJUN ZHAO received the Ph.D. degree in mechanical engineering from Yanshan University, Qinhuangdao, China, in 2019.

His research interests include the electrochemical micromachining, MEMS control technology, and fabrication of micro or nanostructured structure.

LIZHONG XU received the Ph.D. degree in machine design and theory from Yanshan University, China, in 1999.

He is currently a Professor of machine design and theory with Yanshan University. His primary research interests include the area of mechanical transmission, electromagnetic railgun, micro sensors, micro motors, and electromechanical integrated systems.